Stabilization of the Dipole Alignment of Poled Nonlinear Optical Polymers by Ultrastructure Synthesis

Chengzeng Xu, Bo Wu, Olga Todorova, and Larry R. Dalton*

Department of Chemistry, University of Southern California, Los Angeles, California 90089-1062

Yongqiang Shi, Peter M. Ranon, and William H. Steier

Department of Electrical Engineering, University of Southern California, Los Angeles, California 90089-0483

Received March 23, 1993; Revised Manuscript Received June 29, 1993•

ABSTRACT: A new approach to attaining long term and high temperature stability of second-order nonlinear optical effects has been developed. Two side-chain copolymers containing dipole-end cross-linkable chromophore pendants were synthesized from a double-end cross-linkable (DEC) chromophore monomer. The polymer solutions containing a cross-linker were spin cast into optical quality thin films, which were subsequently poled by an electric field, using a corona configuration, and thermally cross-linked. Second-order susceptibilities, $\chi^{(2)}$, on the order of 10^{-7} esu, of the polymer films were measured by the second harmonic generation (SHG) at 1.06-μm fundamental wavelength. The cross-linked films show no SHG signal decay for thousands of hours at room temperature. Thermal stability studies demonstrate that long term stability of the second-order nonlinear optical effects at 125 °C has been realized using the DEC approach.

Introduction

Electrooptic device application of second-order nonlinear optical (NLO) materials requires a large optical nonlinearity and long term stability of the nonlinearity in the working temperature range 60–125 °C. After electric field poling, NLO polymers exhibit large optical nonlinearities. Covalently incorporating NLO moieties into polymers as pendants or part of the backbone is effective in improving the nonlinearity and in imparting good processibility to the NLO materials.[1] Poled polymers, however, exhibit a major disadvantage when compared to inorganic crystals in terms of long term NLO thermostability. In the absence of a poling electric field, the dipole orientation in poled polymers tends to relax to the thermodynamically more stable random structure through polymer chain segmental motions and pendant rotations, leading to the decay of the nonlinearity. Because of this, poled polymers are greatly limited for applications in electrooptics as an alternative to crystals, although they are superior in other aspects such as large nonlinearity, excellent processibility and low cost of fabrication. Therefore, stabilizing the poling-induced noncentrosymmetric lattice is a challenging and critical undertaking.

In addressing this problem, cross-linking reactions have been proven very effective.[2-20] A number of approaches have been explored to realize stabilization of the poling-induced dipole alignment through utilization of cross-linkable polymers. These include thermosetting prepolymers,[2-6] side-chain polymers,[7-12] main-chain polymers,[13-14] and guest–host composites.[15-20] Other methods of stabilizing the poling-induced order include doping NLO chromophores into polymer matrices with high glass transition temperatures (T_g) and attaching the chromophores covalently onto the backbone of high T_g polymers, such as polyimides.[21-23] All of these approaches are somewhat successful in improving the temporal stability of the nonlinearity. So far, however, there has not been a polymer material prepared that meets the aforementioned requirements. Most of the materials still do not possess enough NLO stability, especially at elevated temperatures (e.g., 90–125 °C), and some materials gain the stability at the sacrifice of optical nonlinearity, film quality, or processibility.

To realize acceptable NLO stability without sacrificing the chromophore number density (and hence the second-order optical nonlinearity) and processibility of NLO polymers, we have developed a novel class of double-end cross-linkable (DEC) chromophores.[10] Unlike other chromophores with single-functionality ends, the DEC chromophores have two functionalities at each end. More significantly, the functional groups at the two ends of a DEC chormophore are different in functionality. Noncomplementary functionalities at the two ends make it possible for a DEC monomer to undergo two types of polymerization reactions with different mechanisms (i.e., condensation and addition polymerization). This enables us to synthesize processible polymers that are cross-linkable at the free end of the chromophore pendant. After electric poling and cross-linking, both ends of a chromophore dipole are locked into the polymer network by strong chemical bonds, which is expected to dramatically restrain the motions of the dipoles and therefore minimize relaxation of the noncentrosymmetric order.

Amino–sulfone azobenzene chromophores were used in this paper because of their sizable first molecular hyperpolarizabilities (β) and the flexibility of introducing useful functionalities at the ends of the chromophores. Robello, Williams, and co-workers at Eastman Kodak[24,25] have pioneered the use of this class of chromophores for nonlinear optics. They have introduced a single functionality at each end of an amino–sulfone azobenzene chromophore, from which they have synthesized several head-to-tail main-chain NLO polymers.[24] Using a modified procedure, we have synthesized an amino–sulfone chromophore with one hydroxyl group at each end and synthesized a cross-linkable main-chain NLO polymer with the chromophores randomly bonded in the polymer backbone.[13] In this paper, the detailed design and synthesis of a DEC chromophore monomer with an amino–sulfone donor–acceptor pair as well as its dipole-end cross-linkable polymers will be discussed.

• Abstract published in *Advance ACS Abstracts*, September 1, 1993.

0024-9297/93/2226-5303$04.00/0

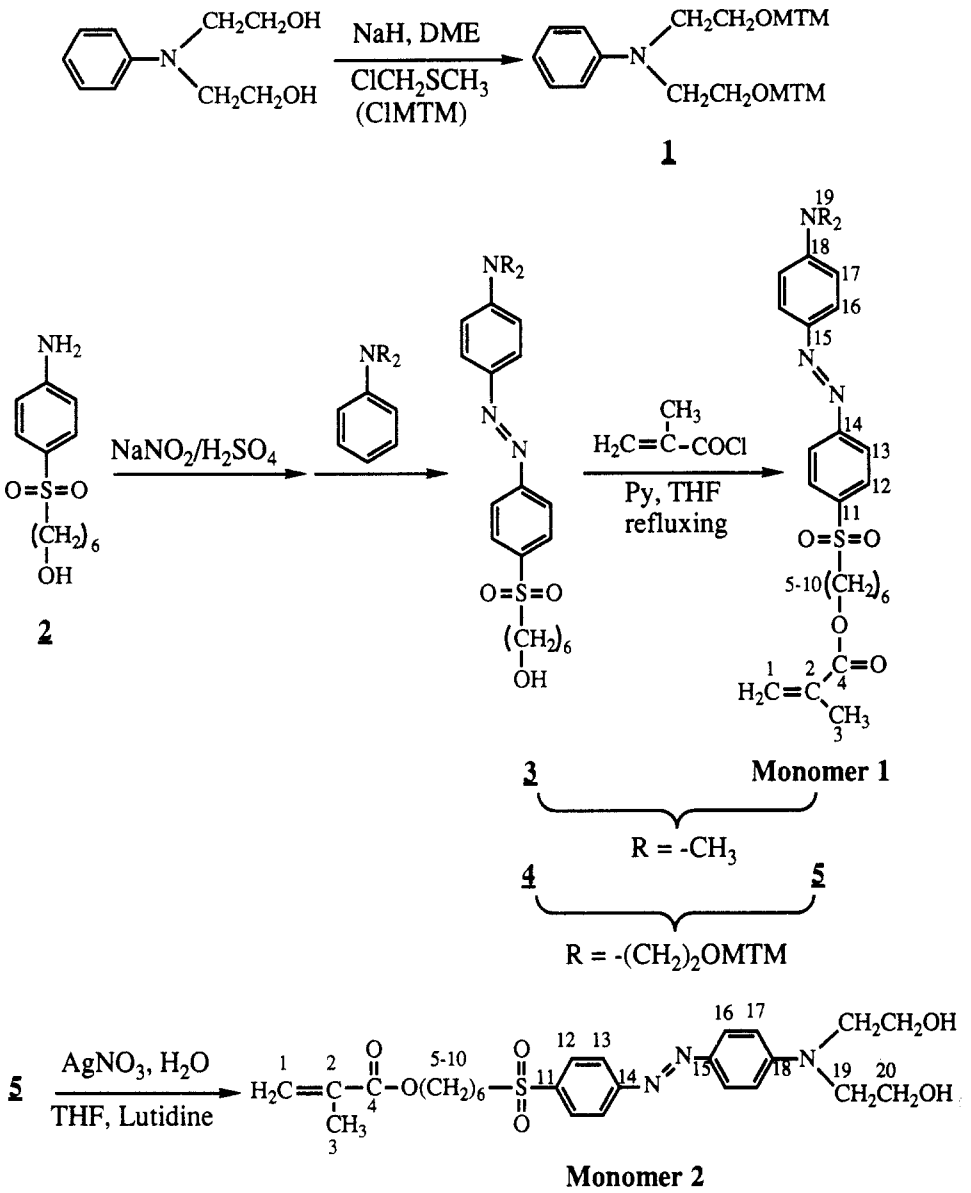

Figure 1. Reaction scheme for the syntheses of monomer 1 and monomer 2.

Experimental Section

General Methods. Conventional ^1H and ^{13}C NMR spectra were taken from a Bruker-250 spectrometer operating at 250 MHz, and two dimensional (2D) NMR spectra were obtained using a Bruker AMX-500 spectrometer operating at 500 MHz. The chemical shifts are referenced to tetramethylsilane (TMS) internal standard. All FTIR spectra were measured with a Perkin-Elmer 1760 FTIR spectrophotometer using pressed KBr pellets. Glass transition temperatures (T_g) and thermal decomposition temperatures (T_d) were determined with Perkin-Elmer DSC-7 and TGA-7 systems, respectively, at a heating rate of 20 °C/min under an argon atmosphere. Elemental analysis was performed by Atlantic Microlab, Inc. Polymer molecular weights were measured by size exclusion chromatography (SEC) using tetrahydrofuran (THF) as the eluent and polystyrene as the standard.

Materials. The solvents used in the moisture sensitive reactions were dried and stored in a drybox before each use. 1,2-Dimethoxyethane (DME) and THF were dried by refluxing with sodium and the indicator benzophenone. Pyridine (Py) was dried by distillation over barium oxide. The comonomers, methyl methacrylate (MMA), methacryloyl chloride, and 2-hydroxyethyl methacrylate (HEMA), were purified by distillation. 4-Aminophenyl 6-hydroxyhexyl sulfone (2) was synthesized according to the published literature procedures.[24] All other starting materials, reagents, and solvents purchased from various chemical companies were analytical reagent grade and were used without further purification unless otherwise noted. The syntheses of monomer 1 and monomer 2 were carried out according to the reaction scheme shown in Figure 1.

***N,N*-Bis(2-((methylthio)methoxy)ethyl)aniline (1).** A three-neck flask containing *N,N*-bis(2-hydroxyethyl)aniline (9.8 g, 54 mmol) was vacuum dried at 60 °C and back-filled with argon. Dry DME was added into the flask under argon, and the solution was cooled to 0 °C in a salt–ice bath. To the stirred solution was added sodium hydride (5.2 g, 0.22 mol). After the solution stopped bubbling, 18 g (0.11 mol) of potassium iodide and then 10.4 g (0.11 mol) of chloromethyl methyl sulfide (ClMTM) were added. After 1 h at 0 °C, the reaction solution was stirred overnight in an unattended ice bath, which gradually reached room temperature. The resulting suspension was poured into 250 mL of water, and the mixture separated into three layers. The aqueous layer (middle layer) and the bottom layer were extracted with ether. The ether portion was washed with brine, dried over anhydrous potassium carbonate, and then concentrated. The pale yellow oil obtained was purified by column chromatography (silica gel; hexanes/ether, 1:4 by volume), affording 8.5 g (53%) of oily product. ^1H NMR ($CDCl_3$): δ 7.21 (t, J = 7.2 Hz, 2H), 6.71 (m, br, 3H), 4.63 (s, 4H), 3.70 (t, J = 6.2 Hz, 4H), 3.60 (t, J = 6.2 Hz, 4H), 2.13 (s, 6H).

4-(Dimethylamino)-4′-((6-hydroxyhexyl)sulfonyl)azobenzene (3). To a stirred, salt–ice cooled aqueous sulfuric acid (6 M, 10 mL) solution containing 4-aminophenyl 6-hydroxyhexyl sulfone (2.0 g, 7.8 mmol) was added dropwise an aqueous sodium nitrite (0.6 g, 8.7 mmol) solution. The reaction temperature was maintained below 5 °C throughout the reaction to prevent the

decomposition of the intermediate diazonium salt. After 15 min of stirring, *N,N*-dimethylaniline (0.95 g, 7.8 mmol) was added, and the resulting red solution was stirred for additional 30 min. Sodium hydroxide (NaOH) (10%) was slowly added to neutralize the reaction mixture to pH = 6. The precipitate formed was filtered out, washed extensively with water and cold ethanol, and vacuum dried. The orange solid (2.48 g, 82%) was further purified by recrystallization from ethanol. ^{1}H NMR ($CDCl_3$): δ 7.98 (m, br, 6H), 6.79 (d, J = 9.0 Hz, 2H), 3.61 (t, J = 6.2 Hz, 2H), 3.15 (m, br, 8H), 1.75–1.37 (m, br, 8H). Anal. Calcd for $C_{20}H_{27}N_3O_3S$: C, 61.70; H, 6.94; N, 10.80; S, 8.23. Found: C, 61.82; H, 7.11; N, 10.76; S, 8.33.

Monomer 1. Methacryloyl chloride (1.1 g, 10.3 mmol) in 5 mL of dry THF was added dropwise to a stirred THF solution (15 mL) of **3** (2.0 g, 5.1 mmol) and dry pyridine (0.8 g, 10.3 mmol). The reaction mixture was refluxed under argon for 14 h and then evacuated to pump out THF. To the residue was added 1% NaOH aqueous solution, and the resulting mixture was extracted three times with chloroform. The chloroform layer was washed three times with brine and dried over anhydrous magnesium sulfate. After evaporating the solvent, the residue was purified by column chromatography (silica gel; chloroform/ethyl acetate, 1:4). After vacuum drying, 1.75 g (75%) of red solid product was obtained. ^{1}H NMR ($CDCl_3$): δ (see Figure 2 for the numbered structure) 7.98 (m, br, 6H, $H_{12,13,16}$), 6.78 (d, J = 9.2 Hz, 2H, H_{17}), 6.07 (s, 1H, H_{1cis}), 5.54 (m, 1H, H_{1tr}), 4.11 (t, J = 6.6 Hz, 2H, H_5), 3.14–3.08 (m, br, 8H, $H_{10,19}$), 1.93 (s, 3H, H_3), 1.65–1.38 (m, br, 8H, H_{6-9}). ^{13}C NMR ($CDCl_3$): δ 167.3 (C_4), 156.2 (C_{14}), 153.1 (C_{18}), 143.4 (C_{15}), 138.1 (C_{11}), 136.3 (C_2), 129.0 (C_{12}), 125.8 (C_{16}), 125.3 (C_1), 122.6 (C_{13}), 111.4 (C_{17}), 64.4 (C_5), 56.2 (C_{10}), 42.2 (C_{19}), 28.2 (C_6), 27.8 (C_8), 25.4 (C_7), 22.6 (C_9), 18.2 (C_3). Anal. Calcd for $C_{24}H_{31}N_3O_4S$: C, 63.02; H, 6.78; N, 9.19; S, 7.00. Found: C, 62.68; H, 6.85; N, 8.92; S, 6.93.

4-[Bis(2-((methylthio)methoxy)ethyl)amino]-4′-((6-hydroxyhexyl)sulfonyl)azobenzene (4). The diazonium salt of 4-aminopropyl 6-hydroxyhexyl sulfone was prepared using the same procedure as that for the preparation of **3**. To this ice cooled diazonium salt solution was added sodium acetate tetrahydrate to adjust the pH to ca. 2. Compound **1** was then added with vigorous stirring, and the solution turned red immediately. The reaction mixture was adjusted to pH 6 by adding 10% NaOH and then extracted with dichloromethane. The organic layer was washed with brine, dried over magnesium sulfate, and concentrated. The resulting red oil was further purified by column chromatography (silica gel; ethyl acetate/hexanes, 3:2). ^{1}H NMR ($CDCl_3$): δ 7.97 (m, br, 4H), 7.89 (d, J = 9.1 Hz, 2H), 6.83 (d, J = 9.2 Hz, 2H), 4.64 (s, 4H), 3.76 (m, br, 8H), 3.59 (t, J = 6.3 Hz, 2H), 3.08 (t, J = 7.6 Hz, 2H), 2.11 (s, 6H), 1.52–1.37 (m, br, 8H). Anal. Calcd for $C_{26}H_{39}N_3O_6S_3$: C, 54.84; H, 6.85; N, 7.38; S, 16.87. Found: C, 54.12; H, 6.70; N, 7.14; S, 16.41.

Compound 5. Methacryloyl chloride (2.9 g, 28.1 mmol) in 10 mL of dry THF was dropped into a stirred THF solution (70 mL) consisting of 8.0 g (14.0 mmol) of **4** and 2.2 g (28.1 mmol) of dry pyridine. The reaction mixture was refluxed under argon for 14 h and then evacuated to pump out THF. The remaining viscous red liquid was dissolved in chloroform and washed with 1% NaOH and brine. The concentrated chloroform solution was loaded onto a column of silica gel and purified by chromatography (ethyl acetate/chloroform, 4:1), affording 6.4 g (71%) of extremely viscous red oil. ^{1}H NMR ($CDCl_3$): δ 7.97 (m, br, 4H), 7.90 (d, J = 9.1 Hz, 2H), 6.83 (d, J = 9.2 Hz, 2H), 6.08 (s, 1H), 5.54 (s, 1H), 4.64 (s, 4H), 4.11 (t, J = 6.6 Hz, 2H), 3.76 (m, br, 8H), 3.12 (t, J = 7.9 Hz, 2H), 2.11 (s, 6H), 1.93 (s, 3H), 1.77–1.37 (m, br, 8H). Anal. Calcd for $C_{30}H_{43}N_3O_6S_3$: C, 56.48; H, 6.81; N, 6.59; S, 15.07. Found: C, 56.19; H, 7.01; N, 6.13; S, 15.04.

Monomer 2. A solution containing **5** (3.9 g, 6.7 mmol), silver nitrate (12.0 g, 70.5 mmol), 2,6-lutidine (4.6 g, 42.3 mmol), THF (32 mL), and water (8 mL) was vigorously stirred overnight at room temperature. THF was pumped out, and chloroform was added. The chloroform solution was washed five times with copper(II) sulfate aqueous solution and then three times with brine. The chloroform solution was dried over magnesium sulfate and concentrated. The orange solid obtained was purified twice by column chromatography (silica gel; ethyl acetate/chloroform/methanol, 9:1:1), yielding 1.9 g (60%) of pure product. ^{1}H NMR ($CDCl_3$): δ (see Figure 1 for the numbered structure of monomer 2) 7.96 (m, br, 4H, $H_{12,13}$), 7.89 (d, J = 8.0 Hz, 2H, H_{16}), 6.82 (d, J = 8.8 Hz, 2H, H_{17}), 6.07 (s, 1H, H_{1cis}), 5.54 (m, 1H, H_{1tr}), 4.10 (t, J = 6.5 Hz, 2H, H_5), 3.96 (t, J = 4.4 Hz, 4H, H_{20}), 3.77 (t, J = 4.3 Hz, 4H, H_{19}), 3.10 (t, J = 7.7 Hz, 2H, H_{10}), 1.92 (s, 3H, H_3), 1.76–1.61 (m, br, 4H, $H_{6,9}$), 1.39 (m, br, 4H, $H_{7,8}$). ^{13}C NMR ($CDCl_3$): δ 167.5 (C_4), 156.1 (C_{14}), 153.0 (C_{18}), 143.6 (C_{15}), 138.2 (C_{11}), 136.3 (C_2), 129.0 (C_{12}), 126.1 (C_{16}), 125.4 (C_1), 122.6 (C_{13}), 112.3 (C_{17}), 64.3 (C_5), 60.4 (C_{20}), 56.3 (C_{10}), 55.2 (C_{19}), 28.2 (C_6), 28.1 (C_8), 25.5 (C_7), 22.6 (C_9), 18.3 (C_3). Anal. Calcd for $C_{26}H_{35}N_3O_6S$: C, 60.31; H, 6.77; N, 8.12; S, 6.19. Found: C, 60.13; H, 6.79; N, 8.04; S, 6.16.

Polymer 1. Into a polymerization tube was placed monomer **1** (0.46 g, 1.0 mmol), MMA (0.30 g, 3.0 mmol), AIBN (3.7 mg, 0.02 mmol), and chloroform (4 mL). The tube was cooled in a dry ice bath, evacuated to 0.05 mmHg and then sealed. The polymerization solution was heated at 60 °C for 48 h, cooled to room temperature and then poured into 60 mL of vigorously stirred methanol. The resulting precipitate was filtered out, washed with methanol, and dried. The polymer was further purified by dissolving in chloroform and reprecipitating in methanol. The product obtained was an orange powder (0.21 g, 27%). ^{1}H NMR ($CDCl_3$): δ 7.94 (m, br, 6H), 6.77 (d, J = 8.6 Hz, 2H), 3.89 (vb, 2H), 3.59 (vb, 12H), 3.13 (vb, 8H), 1.87–0.84 (m, vb). ^{13}C NMR ($CDCl_3$): δ 178.0–177.0 (m), 155.9, 153.3, 143.3, 138.3, 129.1, 126.2, 122.6, 111.7, 64.7, 56.2, 54.2, 52.4, 44.8, 44.5, 40.4, 27.9, 27.7, 25.6, 22.6, 18.8 (m), 16.4 (m).

Polymer 2. Polymer 2 was synthesized using a similar procedure to that for the preparation of polymer 1. A sealed polymerization tube containing 0.35 g (0.68 mmol) of monomer **2**, 0.20 g (2.03 mmol) of MMA, 4.5 mg (0.027 mmol) of AIBN, and 3 mL of dimethyl sulfoxide (DMSO) was heated in a bath at 60 °C for 86 h. The resulting solution was poured into 50 mL of methanol with vigorous stirring to obtain a gel-like solid. The solid was dried in vacuum at 70 °C for 48 h, washed with chloroform, redissolved in DMSO, and then reprecipitated in methanol, yielding 0.25 g (45%) of red powder. ^{1}H NMR (DMSO-d_6): δ 7.94 (m, br, 4H), 7.78 (d, J = 7.5 Hz, 2H), 6.86 (d, J = 7.4 Hz, 2H), 4.84 (br, 2H), 3.81 (vb, 2H), 3.58–3.49 (m, vb), 1.72–0.70 (m, vb). ^{13}C NMR (DMSO-d_6): δ 178.0–177.0 (m), 155.4, 15.20, 142.4, 138.4, 129.0, 125.7, 122.2, 111.5, 58.1, 54.6, 53.3, 51.7, 44.2, 43.9, 27.9, 27.0, 25.0, 22.2, 18.3 (m), 16.1 (m).

Polymer 3. Polymer 3 was synthesized using the above procedure. A polymerization tube containing monomer **2** (0.35 g, 0.68 mmol), MMA (0.14 g, 13.5 mmol), HEMA (0.09 g, 0.68 mmol), AIBN (4.4 mg, 0.027 mmol), and DMSO (3 mL) was vacuum sealed and heated at 60 °C for 86 h. After cooling to room temperature, the resulting solution was poured into 100 mL of vigorously stirred methanol. A gel-like precipitate was formed, which was subsequently dissolved in DMSO and precipitated in methanol again. The precipitate was collected by filtration, washed with methanol and chloroform, and dried, affording 0.32 g (55%) of orange powder. ^{1}H NMR (DMSO-d_6): δ 7.99 (br, 4H), 7.78 (br, 2H), 6.86 (br, 2H), 4.85 (br, 2H, –O*H*), 4.78 (br, 1H, –O*H*), 3.87 (vb), 3.58–3.48 (vb), 1.75–0.71 (vb).

Cross-Linked Film. A dry THF solution containing polymer **2** and the cross-linker (4,4′-diisocyanato-3,3′-dimethoxybiphenyl) in a 1:1 molar ratio was spin cast into a thin film on a glass slide substrate. The film was heated in a sealed oven at 160 °C under argon atmosphere to initiate cross-linking. FTIR was employed to monitor the reaction between the hydroxy and isocyanate groups.

NLO Measurements. Polymer 1 is soluble in chloroform and polymer 2 and polymer 3 are soluble in THF. The polymer solutions, with or without the cross-linker, were filtered through 0.2-μm syringe filters and then spin cast onto indium–tin oxide (ITO) coated glass slides. The films were vacuum dried and stored in a drybox before electric poling and NLO measurement. An ITO-grounded corona-discharge setup, with a tip-to-plane distance of 2.0 cm, was used to pole the films at elevated temperatures. The poling conditions are as follows: (1) for polymer 1 10 kV, 125 °C, and 45 min; (2) for polymer 2 with the cross-linker 5 kV, 140–160 °C, and 2 h; (3) for polymer 3 with the cross-linker 5 kV, 150 °C and 2 h. The film thickness of 0.5–1.5 μm was measured by a Dektak IIA profiler.

The absorption spectra of the polymer films, before and after electric filed poling, were measured with a Varian Cary 2415 spectrophotometer operating in the wavelength range 300–2500 nm.

A Spectro-Physics DCR-11 mode-locked, Q-switched Nd:YAG laser ($\lambda = 1.064\ \mu m$) with a pulse width of <10 ns and repetition rate of 10 Hz was used as the fundamental source. A Y-cut quartz crystal ($d_{11}^r = 0.5$ pm/V) was used as the reference. The quartz crystal was at a ca. 6° angle to the incident laser beam, and the sample film was at a 45° angle to the incident beam.

The effective SHG coefficient of a NLO polymer, d_{eff}^p, can be calculated from the comparison of the second harmonic signals between the reference and the polymer sample by using the following equation:

$$d_{eff}^p = d_{11}^r \times \sqrt{\frac{I_p}{I_r}} \frac{n_{2\omega,p} L_{c,r} \sqrt{T_{2\omega,r}}\, t_{\omega,r}^2}{n_{2\omega,r} L_{c,p} \sqrt{T_{2\omega,p}}\, t_{\omega,p}^2} \frac{e^{\alpha L/4} \sqrt{1+\left(\frac{\alpha L}{2\pi}\right)^2 \left(\frac{L_{c,p}}{L}\right)^2}}{\sqrt{sinh^2\left(\frac{\alpha L}{4}\right) + sin^2\left(\frac{\pi L}{2L_{c,p}}\right)}} \quad (1)$$

where I is the SHG intensity, $n_{2\omega}$ is the refractive index at the second harmonic (SH) wavelength, L_c is the coherence length, $T_{2\omega}$ is the transmittance at the SH wavelength, t_ω is the amplitude transmission coefficient at fundamental wavelength, α is the absorption coefficient of the polymer film at 2ω, L is the thickness of the polymer film, and the subscripts p and r denote polymer sample and reference, respectively. The refractive indices were measured at three wavelengths using a four-zone averaging method with an ellipsometer.

For the p-polarized incident fundamental beam used in our measurement, d_{33} of the polymer sample can be obtained after geometry correction by using the equation

$$d_{eff}^p = \left[\left(\frac{1}{3}\cos^2\theta_\omega + \sin^2\theta_\omega\right)\sin\theta_{2\omega} + \frac{2}{3}\cos\theta_\omega \sin\theta_\omega \cos\theta_{2\omega}\right] d_{33} \quad (2)$$

where θ_ω and $\theta_{2\omega}$ are transmitted angles of the fundamental and second harmonic beams in the polymer film.

To study the temporal stability of second-order optical nonlinearities at room temperature after the poling electric field was removed, the polymer films were stored in a drybox to minimize possible pollution caused by chemicals or dust in the laboratory environment. To study the long term NLO stability at elevated temperatures, the polymer films were baked continuously in the ovens under air atmosphere at 90 and 125 °C, respectively. The temperature reading error is ±5 deg. The SHG coefficients at various time intervals were measured.

Results and Discussion

Synthesis of Materials. The synthetic scheme of the chromophore monomers is shown in Figure 1. To attach different functionalities to the two ends of a chromophore dipole, the two hydroxy groups in *N,N*-bis(2-hydroxyethyl)aniline were protected and later deprotected using a literature method.[26] (Methylthio)methane (MTM) was chosen as the protecting group for its relative stability to the acidic conditions used in the diazonium coupling reactions. In the synthesis of 4, sodium acetate was added to the diazonium salt solution to adjust the pH to ca. 2 before 1 was added to prevent the cleavage of the protecting group in a strong acid.

All the intermediate compounds and monomers obtained were pure and gave satisfactory NMR and elemental analysis results. Using the 2D NMR technique and with the assistance of other NMR techniques such as homonuclear decoupling, 2D long range correlation, and APT (attached proton test), we were able to assign the ^1H and ^{13}C peaks. The assignments of the ^1H and ^{13}C peaks for monomer 1 and monomer 2 (see Figure 1) are listed in the Experimental Section. These NMR assignments together with the elemental analysis data validate the structures of the monomers synthesized.

All three polymers were synthesized by radical addition polymerization with AIBN as the initiator. DMSO was used as the solvent for the syntheses of polymer 2 and polymer 3 because the oligomers formed were not soluble in chloroform and precipitates were formed during the polymerization in chloroform, which led to low molecular weights. The formation of the polymers was demonstrated by FTIR, NMR, and size exclusion chromatography (SEC). The characteristic methacrylate FTIR band at 1636 cm^{-1} and NMR peaks (^1H 6.07, 5.54, 1.93 ppm; ^{13}C 125.3, 136.3, 18.2 ppm) from the monomers completely vanished after the polymerization while other non-methacrylate FTIR bands and NMR peaks were retained. The new ^1H and ^{13}C NMR peaks of saturated hydrocarbons also provided evidence for the formation of the polymers. The number average molecular weight of polymer 1 is 44 000. The number average molecular weight of polymer 2 is measured to be around 5000. While the molecular weight of polymer 2 is relatively low, the number average molecular weight of polymer 3 is surprisingly high (900 000). The polydispersities for all the three polymers are in the range 2–4. For polymer 1, the molar ratio of the chromophore to MMA in the copolymer was estimated from NMR data to be 1:3.7, which was somewhat off the monomer input ratio of 1:3. This can be explained by the steric hindrance of the bulky chromophore monomer, which reduces the copolymerization reactivity. For polymer 3, the molar ratio of the chromophore monomer to HEMA in the copolymer was estimated from the integration values of the hydroxy (–OH) ^1H NMR peaks at 4.85 (~2H) and 4.78 ppm (~1H), respectively. The 2:1 ratio estimated from the NMR spectrum implies that the molar ratio of the chromophore to HEMA in the copolymer is 1:1 because each chromophore monomer consists of two hydroxy groups.

A unique feature of the structure of monomer 2 (see Figure 1) is that it has one methacrylate group, which can be polymerized by radical reactions, at one end of the chromophore and two hydroxy groups, which can be polymerized by condensation reactions, at the other end. Each type of polymerization (radical or condensation) leads to a side-chain polymer having cross-linkable functional groups at the free ends of the chromophore pendants. For example, as shown in Figure 2, polymer 2 was synthesized from copolymerization of monomer 2 and MMA by radical polymerization. This side-chain polymer is soluble in THF and other organic solvents and can be processed into optical quality thin films by spin casting. A film of polymer 2 consisting of the cross-linker (XL), 4,4′-diisocyanato-3,3′-dimethoxybiphenyl, was poled by an electric field and cross-linked by the condensation reactions between the hydroxy groups and isocyanate groups. Cross-linking at the ends of the chromophore pendants, which can be either interchain or intrachain reactions, forms three dimensional (3D) networks and locks in the dipole alignment by fixing both ends, as illustrated by the simplified diagram in Figure 3. Similarly, polymer networks with dipole alignment locked in can be formed from polymer 3.

The cross-linking reaction of polymer 2 with the cross-linker (XL) was monitored by FTIR spectra. Figure 3 shows the spectra measured before and after thermal curing of the film in an oven at 160 °C. The relative intensity of the isocyanate peak instead of the hydroxy peak was used to monitor the cross-linking reaction because the latter is too broad to be well defined, although a peak shift was observed after curing. The characteristic peak of the isocyanate group at 2248 cm^{-1} decreased after the

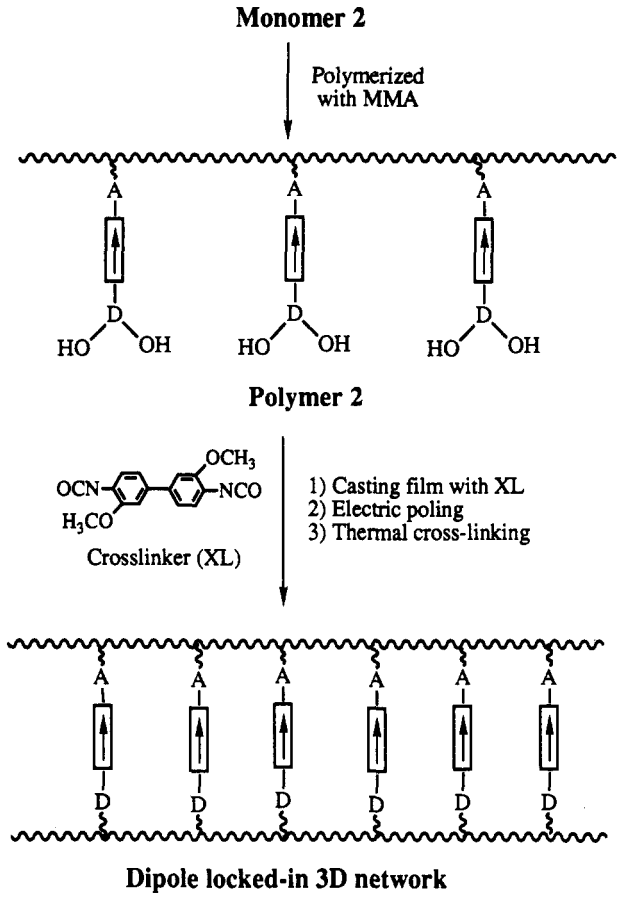

Figure 2. Simplified schematic diagram for the formation of the 3D polymer network with dipole alignment locked in through cross-linking reaction.

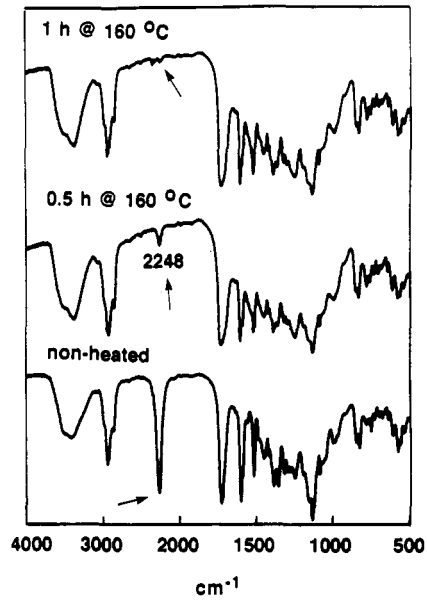

Figure 3. FTIR spectra of polymer 2 with the cross-linker, before and after thermal curing.

curing and completely disappeared after 1 h. The cured polymer films peeled off the slides are not soluble in organic solvents (including DMSO), which also indicates cross-linking of the film.

Thermal properties were characterized with DSC and TGA. The thermal decomposition temperature (T_d) was recorded when the polymer started to lose weight. The glass transition temperature (T_g) and T_d for polymer 1 are 120 and 265 °C, respectively. The DSC scans of the non-cross-linked polymer 2 and polymer 3 samples show similar glass transitions around 130 °C, while the scans of the

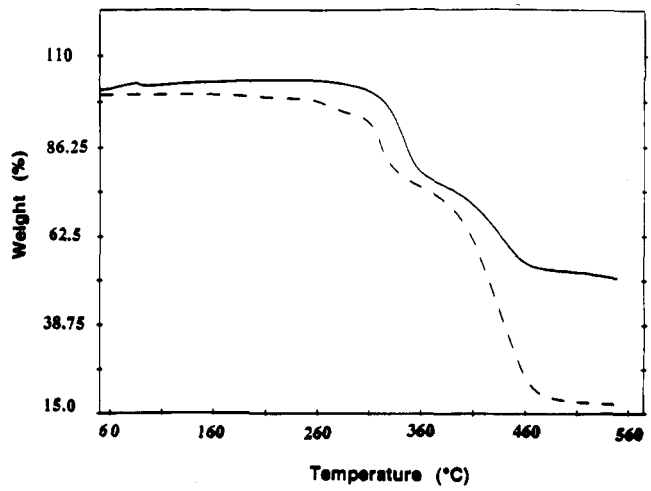

Figure 4. TGA curves of the non-cross-linked (broken line) and cross-linked (solid line) polymer 2 samples.

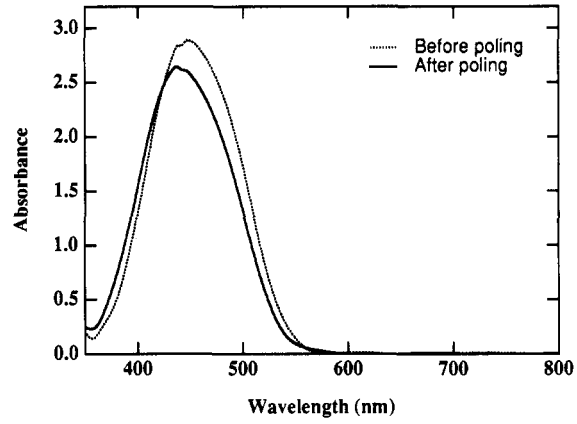

Figure 5. Absorption spectra of the polymer 2 film coated on an ITO glass substrate, before and after electric poling.

cross-linked samples show no detectable transitions from 50 to 250 °C. Figure 4 shows the TGA curves of polymer 2 samples. The T_d of the non-cross-linked polymer 2 is around 260 °C, which is typical for methacrylate polymers. The cross-linked sample, however, shows no weight loss below 315 °C. These results demonstrate that the thermal stability of polymeric materials can be improved by cross-linking. Both non-cross-linked and cross-linked polymer 3 samples exhibit similar thermal decomposition behaviors.

NLO Properties. The polymer films have no detectable absorption between 800 and 2500 nm. The spectra between 300 and 800 nm shown in Figure 5 were obtained from the same film of polymer 3 with the cross-linker, before and after poling. The charge transfer absorption peaks due to the chromophore in all the three polymers are virtually at the same wavelength ($\lambda_{max} \approx 440$ nm). After electric poling, an absorbance decrease was observed for all the films. This decrease is caused by the alignment of the chromophore dipoles[27] instead of the chromophore structure damage because this spectrum change is reversible upon thermal annealing. The comparison between the FTIR spectra measured before and after electric poling shows that the characteristic peaks and the spectral patterns of the chromophores remain unchanged. This also indicates that the polymers survive the high poling temperature and electric field without being structurally damaged.

The poled polymer films exhibit large second-order optical nonlinearities as measured by the second harmonic generation at 1064 nm fundamental wavelength. Using the quartz crystal as a reference standard, the SHG

Table I. Optical Properties of NLO Polymers

polymer	refractive index n(532 nm)	refractive index n(1064 nm)	abs peak (nm)	$10^7\chi^{(2)}$(532 nm) (esu)	$10^7\chi^{(2)}$(800 nm) (esu)
NXLP1	1.717	1.571	437	5.3	2.0
XLP2	1.811	1.639	437	2.9	1.2
XLP3	1.719	1.557	438	2.2	0.8

coefficients (d_{33}) of the polymers were calculated with eq 1. Because of the absorption tail at the second harmonic wavelength (532 nm), the refractive indices (n_ω and $n_{2\omega}$) were obtained indirectly by a four-zone-averaging method using the well-known Sellmeier equation.[28] The second-order nonlinear susceptibility, $\chi^{(2)}$, was then calculated by $\chi^{(2)} = 2d_{33}$. Table I lists some optical properties of polymer 1 (NXLP1) and the cross-linked polymer 2 (XLP2) and polymer 3 (XLP3). The calculated $\chi^{(2)}$ values for NXLP1 and XLP2 are 5.3×10^{-7} and 2.9×10^{-7} esu, respectively. The $\chi^{(2)}$ value for NXLP1 is nearly twice as large as that of XLP2. This can be rationalized by the isotropic-model equation, $\chi^{(2)} = Nf(2\omega)f^2(\omega)\beta\langle\cos^3\theta\rangle$, where N is the chromophore number density, $f(\omega)$ and $f(2\omega)$ are the local field factors, and $\langle\cos^3\theta\rangle$ is the poling alignment factor. The chromophore number density (N) in XLP2 is lower because of the addition of the cross-linker. The poling efficiency, as described by $\langle\cos^3\theta\rangle$, may also be lower because the cross-linking reaction that takes place during the poling process can restrain the segmental motions of the polymer chains. It should be noted that the $\chi^{(2)}$ values measured at 532-nm second harmonic wavelength are resonance enhanced because of the absorption tail at this wavelength. Using the isotropic-model equation the $\chi^{(2)}$ values at 800 nm wavelength were extrapolated from the measured $\chi^{(2)}$ values at 532 nm. The calculated $\chi^{(2)}$(800 nm) values of the three polymers are given in Table I. Clearly, the off-resonance $\chi^{(2)}$ values are smaller than those resonance enhanced ones, i.e., $\chi^{(2)}$(532 nm).

The temporal stability of polymer 2 before and after cross-linking was studied by monitoring the SHG signal as a function of time after the poling electric field was removed. It should be noted that $d(0)$ was measured at 0.5 h after the poling field was turned off to prevent influence of the surface charge produced during corona poling. Figure 6 depicts the comparison of the NLO stability between the cross-linked and non-cross-linked polymer 2 samples at room temperature. As expected, the SHG signal of the cross-linked sample shows no decay over thousands of hours. The nonlinearity of the non-cross-linked sample, on the other hand, decays slowly and then stabilizes at ca. 60% of the initial value.

To study the long term NLO thermostability, the cross-linked films of polymer 2 (XLP2) and polymer 3 (XLP3) were baked continuously at 90 and 125 °C and the SHG d coefficients were measured as a function of time. Figure 7 shows the temporal behaviors of second-order optical nonlinearities of XLP2 and XLP3 at 90 °C. As can be seen, both XLP2 and XLP3 exhibit excellent long term thermostability of NLO activities; 85–90% of the original SHG signal of XLP2 is still retained after 2500 h of baking at 90 °C, and no NLO decay was observed for XLP3 for more than 1000 h. Long term NLO thermostability was also observed at 125 °C. XLP3 shows exceptional stability (Figure 8); within experimental error no SHG signal decay was observed over a period of 200 h. The improvement in thermal NLO stability from XLP2 to XLP3 can be attributed to the higher cross-linking density and more rigid network of the latter, facilitated by the introduction of cross-linking sites onto the backbone.

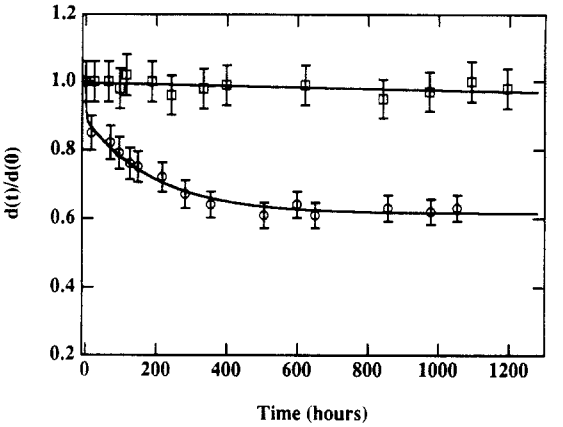

Figure 6. Plot of normalized SHG d coefficients of the cross-linked (square) and non-cross-linked (circle) polymer 2 films as a function of time at room temperature. The solid lines are from least-squares curve fittings.

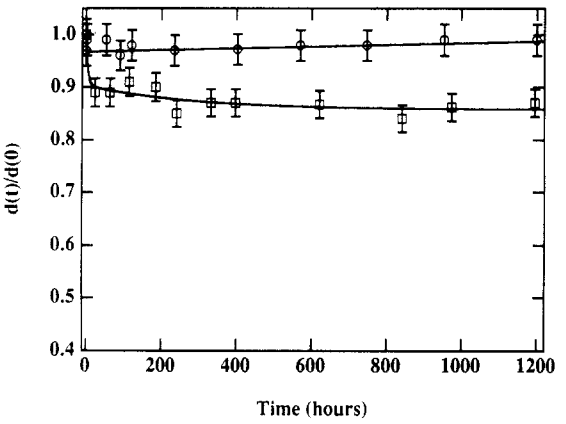

Figure 7. Temporal NLO stability of the cross-linked polymer 2 (squares) and polymer 3 (circles) films at 90 °C.

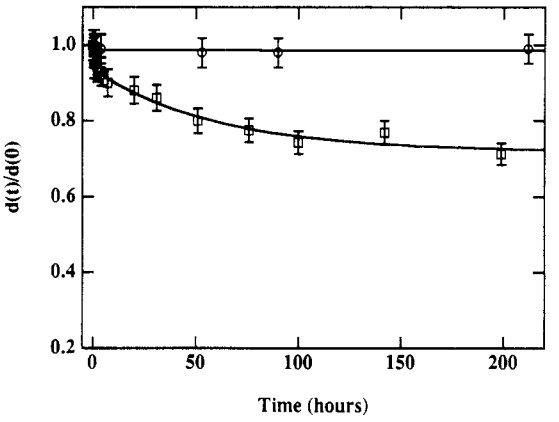

Figure 8. Temporal NLO stability of the cross-linked polymer 2 (squares) and polymer 3 (circles) films at 125 °C.

The temporal NLO stability results demonstrate that the electric field poling-induced macroscopic order can indeed be stabilized by cross-linking reactions using the DEC approach. Two factors may contribute to the excellent temporal and thermal NLO stability: (1) High cross-linking density can be realized in the DEC polymers because of the large number density of the cross-linking sites and the small steric hindrance for the cross-linking reactions to occur, and (2) both ends of the chromophore dipole are locked into the polymer network by strong chemical bonds, which greatly limits the rotation and torsional flexibility of the chromophore unit. Further improvements can be made by introducing large-β chromophores to optimize $\chi^{(2)}$ and by reducing the length of the flexible hydrocarbon chains to increase the rigidity of

the polymer network. Nevertheless, in virtually every category of polymeric electrooptic device requirements, such as large nonlinearity, high NLO stability, ease of processibility, and good film quality, the DEC polymers synthesized have already exhibited advantages and great potential for use in the fabrication of polymer–semiconductor hybrid devices.[29]

Conclusion

We have developed a novel class of NLO chromophores, namely, double-end cross-linkable (DEC) chromophores. By using DEC chromophore monomers, we have synthesized two polymers that have cross-linkable groups at the free ends of the chromophore pendants. These polymers are soluble in common organic solvents and can be spin cast into optical quality thin films. The poled, cross-linked polymer films of the DEC polymers exhibit large second-order optical nonlinearities and long term NLO stability even at 125 °C. The generalized DEC scheme can be extended to prepare polymeric materials with improved nonlinearities (by using large-β chromophores) and other secondary properties necessary for device applications.

Acknowledgment. This research was supported by the Air Force Office of Scientific Research under Contracts F49620-91-0270 and F49620-91-0054, the National Science Foundation Grant DMR-9107806, and the National Center for Integrated Photonic Techology. We gratefully thank Dr. Dimo Dimov and Professor T. E. Hogen-Esch as well as Mark W. Becker for the SEC measurements.

References and Notes

(1) Prasad, P. N.; Williams, D. J. *Introduction to Nonlinear Optical Effects in Molecules and Polymers*; John Wiley & Sons: New York, 1991 (see also references therein).
(2) Eich, M.; Reck, B.; Yoon, D. Y.; Willson, C. G.; Bjorklund, G. C. *J. Appl. Phys.* **1989**, *66*, 3241.
(3) Jungbauer, D.; Reck, B.; Tweig, R.; Yoon, D. Y.; Willson, C. G.; Swalen, J. D. *Appl. Phys. Lett.* **1990**, *56*, 2610.
(4) Shi, Y.; Steier, W. H.; Chen, M.; Yu, L. P.; Dalton, L. R. *Appl. Phys. Lett.* **1992**, *60*, 2577.
(5) Chen, M.; Dalton, L. R.; Yu, L. P.; Shi, Y.; Steier, W. H. *Macromolecules* **1992**, *25*, 4032.
(6) Jungsbauer, D.; Reck, B.; Tweig, R.; Yoon, D. Y.; Willson, C. G.; Swalen, J. D. *J. Appl. Phys.* **1991**, *69*, 8011.
(7) Chen, M.; Yu, L. P.; Dalton, L. R.; Shi, Y.; Steier, W. H. *Macromolecules* **1991**, *24*, 5421.
(8) Yu, L. P.; Chan, W.; Dikshit, S.; Bao, Z.; Shi, Y.; Steier, W. H. *Appl. Phys. Lett.* **1992**, *60*, 1655.
(9) Shi, Y.; Steier, W. H.; Yu, L. P.; Chen, M.; Dalton, L. R. *Appl. Phys. Lett.* **1991**, *58*, 1131.
(10) Xu, C.; Wu, B.; Dalton, L. R.; Shi, Y.; Ranon, P. M.; Steier, W. H. *Macromolecules* **1992**, *25*, 6714.
(11) Park, J.; Marks, T. J.; Yang, J.; Wong, G. K. *Chem. Mater.* **1990**, *2*, 229.
(12) Jin, Y.; Carr, S. H.; Marks, T. J.; Lin, W.; Wong, G. K. *Chem. Mater.* **1992**, *4*, 963.
(13) Xu, C.; Wu, B.; Dalton, L. R.; Ranon, P. M.; Shi, Y.; Steier, W. H. *Macromolecules* **1992**, *25*, 6716.
(14) Ranon, P. M.; Shi, Y.; Steier, W. H.; Xu, C.; Wu, B.; Dalton, L. R. *Appl. Phys. Lett.* **1993**, *62*, 2605.
(15) Hubbard, M. A.; Marks, T. J.; Yang, J.; Wong, G. K. *Chem. Mater.* **1989**, *1*, 167.
(16) Mandal, B. K.; Chen, Y. M.; Lee, J. Y.; Kumar, J.; Tripathy, S. K. *Appl. Phys. Lett.* **1991**, *58*, 2459.
(17) Allen, S.; Bone, D. J.; Carter, N.; Ryan, T. G.; Sampson, R. B.; Devonald, D. P.; Hutchings, M. G. In *Organic Materials for Nonlinear Optics II*; Hann, R. A., Bloor, D., Eds.; The Royal Society of Chemistry: London, 1991; p 235.
(18) Hubbard, M. A.; Marks, T. J.; Lin, W.; Wong, G. K. *Chem. Mater.* **1992**, *4*, 965.
(19) Jeng, R. J.; Chen, Y. M.; Jain, A. K.; Kumar, J.; Tripathy, S. K. *Chem. Mater.* **1992**, *4*, 972.
(20) Jeng, R. J.; Chen, Y. M.; Jain, A. K.; Kumar, J.; Tripathy, S. K. *Chem. Mater.* **1992**, *4*, 1141.
(21) Wu, J. W.; Valley, J. F.; Ermer, S.; Binkley, E. S.; Kenney, J. T.; Lipscomb, G. F.; Lytel, R. *Appl. Phys. Lett.* **1991**, *58*, 225.
(22) Wu, J. W.; Binkley, E. S.; Kenney, J. T.; Lytel, R.; Garito, A. F. *J. Appl. Phys.* **1991**, *69*, 7366.
(23) Lin, J. T.; Hubbard, M. A.; Marks, T. J.; Lin, W.; Wong, G. K. *Chem. Mater.* **1992**, *4*, 1148.
(24) Köhler, W.; Robello, D. R.; Willand, C. S.; Williams, D. J. *Macromolecules* **1991**, *24*, 4589.
(25) Ulman, A.; Willand, C. S.; Köhler, W.; Robello, D. R.; Williams, D. J.; Handley, L. *J. Am. Chem. Soc.* **1990**, *112*, 7083.
(26) Corey, E. J.; Bock, M. G. *Tetrahedron Lett.* **1975**, 3269.
(27) Mortazavi, M. A.; Knoesen, A.; Kowel, S. T.; Higgins, B. G.; Dienes, A. *J. Opt. Soc. Am. B* **1989**, *6*, 733.
(28) Azzam, R. M. A.; Bashara, N. M. *Ellipsometry and Polarized Light*; North-Holland Physics Publishing: Amsterdam, 1987.
(29) Shi, Y.; Ranon, P. M.; Steier, W. H.; Xu, C.; Wu, B.; Dalton, L. R. *Appl. Phys. Lett.*, in press.